Mon. Not. R. Astron. Soc. **000**, 000–000 (0000) Printed 29 May 2015 (MN LATEX style file v2.2)

Dependence of the Cosmic Microwave Background Lensing Power Spectrumon the Matter Density

Z. Pan, [1⋆] L. Knox,[1]† and M. White,[2]‡
[1] *Department of Physics, University of California,One Shields Avenue, Davis, CA, USA 95616*
[2] *Department of Physics and Astronomy, University of California, Berkeley, CA, USA 94720*

arXiv:1406.5459v2 [astro-ph.CO] 28 May 2015

29 May 2015

ABSTRACT
The anisotropies in the cosmic microwave background (CMB) provide our best laboratory for testing models of the formation and evolution of large-scale structure. The rich features in the cosmic microwave background anisotropy spectrum, in combination with highly precise observations and theoretical predictions, also allow us to simultaneously constrain a number of cosmological parameters. As observations have progressed, measurements at smaller angular scales have provided increasing leverage. These smaller angular scales provide sensitive measures of the matter density through the effect of gravitational lensing. In this work we provide an analytic explanation of the manner in which the lensing of CMB anisotropies depends on the matter density, finding that the dominant effect comes from the shape of the matter power spectrum set by the decay of small-scale potentials between horizon crossing and matter-radiation equality.

Key words: cosmology – cosmology:cosmic microwave background – cosmology: observations – large-scale structure of universe

1 INTRODUCTION

Observations of the cosmic microwave background (CMB) temperature power spectrum have provided us with highly precise determinations of cosmological parameters (Planck Collaboration XVI 2013; Hinshaw et al. 2013). These determinations are widely used to aid in the interpretation of other cosmological observables and to search for possible failures of the standard cosmological model that may point us toward new physics. Highly precise inferences are possible due to the way the rich features in the power spectrum depend on the underlying model parameters, the ability to compute the spectrum with high accuracy (Seljak et al. 2003) and recent high-precision measurements of the anisotropy (Planck Collaboration I 2013). Given the widespread use of these parameter inferences, it is important that we acquire a physical understanding of how the parameter constraints arise. Fortunately, the anisotropies arise from relatively simple physical processes so such an understanding is possible (Hu & Dodelson 2002).

As emphasized by Hou et al. (2014), gravitational lensing of the CMB temperature anisotropy power spectrum allows for constraints on the matter density from measurements of the small-scale (high ℓ) portion of the spectrum. Such precise measurements are now becoming available thanks to the Planck (Planck Collaboration I 2011), South Pole Telescope (SPT; Carlstrom et al. 2011) and Atacama Cosmology Telescope (ACT; Sievers et al. 2013) collaborations. However, a physical understanding of the dependence of the CMB lensing power spectrum on the matter density has so far been missing. In this article we provide an understanding of this dependence, within the context of the ΛCDM model. We will find that it is the decay of the potentials after horizon crossing due to the presence of radiation which drives the majority of the dependence and give a simple scaling relation which captures this dependence.

In Section 2 we review the origin of the sensitivity of large-angular scale CMB temperature measurements to the physical matter density, $\omega_m \equiv \Omega_m h^2$. In Section 3 we introduce the lensing potential power spectrum and the basic equations we will use. With those preliminaries, we go on in Section 4 to demonstrate qualitatively and quantitatively the origin of the sensitivity of the CMB lensing potential power spectrum to ω_m. We present our major conclusions in Section 5.

⋆ Email: zhpan@ucdavis.edu
† Email: lknox@ucdavis.edu
‡ Email: mwhite@berkeley.edu

© 0000 RAS

2 THE SPECTRUM BELOW $\ell = 1000$ AND ω_M

The rich structure in the first few acoustic peaks allows us to simultaneously constrain a number of cosmological parameters, including the matter density. Here we briefly review the physics behind these constraints (see e.g. Peacock 1999; Liddle & Lyth 2000; Dodelson 2003, for textbook discussions).

The peaks in the CMB spectrum arise from gravity-driven acoustic oscillations in the primordial, baryon-photon plasma before recombination. For nearly scale-invariant, adiabatic fluctuations the baryon-photon momentum density ratio, R, causes the fluid to oscillate about an offset value, leading to a modulation in the heights of the power spectrum features with enhanced compression (odd) and diminished rarefaction (even) peaks. Physically, the baryons provide a "weight" in the baryon-photon fluid, making it easier to fall into potential wells but harder to climb out.

In contrast the effects of photon self-gravity cause an enhancement of the fluctuations for $\ell \gtrsim 10^2$. This effect is most easily understood by considering the evolution of an overdensity in a potential well as it enters the (sound) horizon and begins to collapse. Since the fluid has pressure, supplied by the photons, it is hard to compress and the infall into the potential is slower than free-fall. Since the overdensity is growing slowly the potential begins to decay due to the expansion of the Universe. The time for the photons to reach their state of maximum compression is the same time scale for the decay of the potential, and the compressed photons do not have a strong potential to work against as they climb back out. Thus the potential decay provides a near-resonant driving and leads to a large[1] increase in power (Hu & White 1996).

The boost from the in-phase potential decay is larger the more the self-energy of the baryon-photon fluid contributes to the total potentials, i.e. the earlier in time and the smaller the (stabilizing) dark matter contribution to the potentials. The boost thus imprints a dependence on the matter density[2], in a similar way to the peak in the matter power spectrum except that the fluctuations in the CMB increase to smaller scales. The matter density can thus be constrained by the heights of the higher order peaks once enough peaks are seen to disentangle the confounding effects of baryon loading and tilt of the initial spectrum.

Since much of the constraining power of the amplitude comes from measurements of the anisotropy with $\ell \gtrsim 10^2$, the dependence of these multipoles on ω_m at fixed A_s implies that inferences of A_s at fixed C_ℓ also depend on ω_m, though in the opposite manner.

[1] In the absence of neutrinos, and if the self-gravity of the baryon-photon fluid dominates the potentials, the amplitude of the oscillation is enhanced by 2Ψ on top of the $-\Psi/3$ plateau at large scales. In popular models the increase of a factor of 5 (from $-\Psi/3$ to $5\Psi/3$) is slightly tempered by the inclusion of neutrinos and further diminished by the stabilizing presence of dark matter.

[2] Or epoch of equality. We shall assume that the radiation density is known, so that equality depends primarily on ω_m.

3 INTRODUCTION TO THE LENSING POWER SPECTRUM

We begin with a brief review of gravitational lensing of the CMB. For details see e.g. the review by Lewis & Challinor (2006). Gradients in the gravitational potential, Φ, distort the trajectories of photons traveling to us from the last scattering surface. The deflection angles, in Born approximation, are $\mathbf{d} = \nabla\phi$, where the lensing potential, ϕ, is a weighted radial projection of Φ. Among other effects, these deflections alter the CMB temperature power spectrum. Regions that are magnified have power shifted to lower ℓ. Regions that are demagnified have power shifted to higher ℓ. The net effect of averaging over these regions is a smoothing out of the peaks and troughs, and a softening of the exponential fall off of the unlensed damping tail to a power law (set by the projected potential power spectrum and the rms of the temperature gradient).

The key quantity for calculating the impact of lensing on the temperature power spectrum is the angular power spectrum of the projected potential, $C_\ell^{\phi\phi}$, which we also call the lensing power spectrum. Taking advantage of the Limber approximation (Limber 1953), it can be written as a radial integral over the three dimensional gravitational potential power spectrum P_Φ

$$\ell^4 C_\ell^{\phi\phi} \simeq 4\int_0^{\chi_\star} \mathrm{d}\chi\ (k^4 P_\Phi)\left(\frac{\ell}{\chi}; a\right)\left[1-\frac{\chi}{\chi_\star}\right]^2, \qquad (1)$$

where χ is the comoving distance from the observer, $a = a(\chi)$, a $\star$ subscript indicates the last scattering surface, $(1-\chi/\chi_\star)^2$ is the lensing kernel, and the power spectrum P_Φ is defined as

$$\left\langle \Phi(\mathbf{k}; a)\Phi^\star(\mathbf{k}'; a)\right\rangle = P_\Phi(k; a)\delta^{(D)}(\mathbf{k}-\mathbf{k}'). \qquad (2)$$

To calculate P_Φ we assume a power-law primordial power spectrum $P_\Phi^p(k)$,

$$\frac{k^3}{2\pi^2}P_\Phi^p(k) = A_s\left(\frac{k}{k_0}\right)^{n_s-1}, \qquad (3)$$

where k_0 is an arbitrary pivot point, A_s and n_s are the primordial amplitude and power law index respectively. There are two conventions for the choice of the pivot point k_0: $0.002\,\mathrm{Mpc}^{-1}$ (constraints from WMAP[3]) and $0.05\,\mathrm{Mpc}^{-1}$ (CAMB[4]). With our assumption of a power-law spectrum the two amplitudes are related by

$$A_s(\mathrm{CAMB}) = A_s(\mathrm{WMAP9}) \times 2.5^{n_s-1}. \qquad (4)$$

We adopt the CAMB convention in this paper and henceforth write $A_s(\mathrm{CAMB})$ as A_s. For many of our formulae we shall additionally approximate n_s by 1, thus rendering the distinction moot.

The gravitational potential at late times, $\Phi(k, a)$, is related to the primordial potential $\Phi^p(k)$ by (e.g. Kodama & Sasaki 1984)

$$\Phi(k, a) = \frac{9}{10}\Phi^p(k)T(k)g(a), \qquad (5)$$

where the potential on very large scales is suppressed by a

[3] `http://lambda.gsfc.nasa.gov`

[4] `http://camb.info`

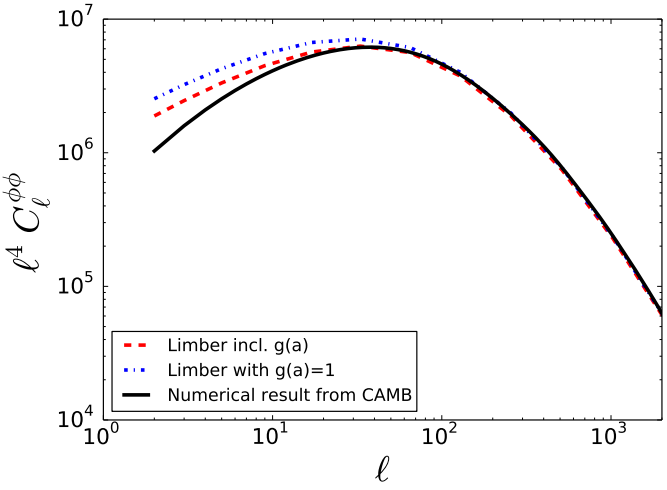

Figure 1. The lensing power spectrum calculated from CAMB (solid line), calculated with Limber approximation (dashed line) and calculated with Limber approximation and setting $g(a) = 1$ (dash-dotted line).

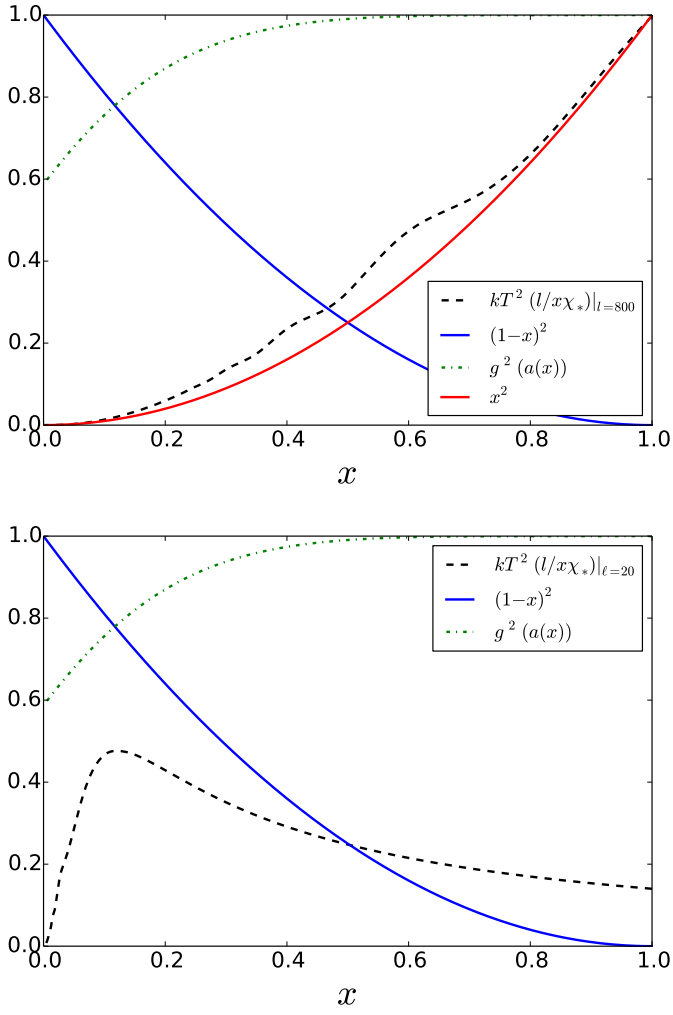

Figure 2. Factors in the integrand of the lensing power spectrum for large $\ell = 800$ (upper panel) and small $\ell = 20$ (lower panel).

factor 9/10 through the transition from radiation domination to matter domination. For modes which enter the horizon during radiation domination when the dominant component has significant pressure ($p \approx \rho/3$) the amplitude of perturbations cannot grow and the expansion of the Universe forces the potentials to decay. For modes which enter the horizon after matter-radiation equality (but before dark energy domination) the potentials remain constant. The transfer function $T(k)$ takes this into account, being unity for very large scale modes and falling approximately as k^{-2} for small scales. Once the cosmological constant starts to become important the potentials on all scales begin to decay. This effect is captured by the growth function, $g(a)$, which is unity during matter domination. With these definitions

$$(k^4 P_\Phi)(k;a) = \frac{81\pi^2}{50} A_s\; g^2(a)\; kT^2(k) \left(\frac{k}{k_0}\right)^{n_s-1}. \qquad (6)$$

With these pieces in place, we now examine the accuracy of the Limber approximation. Fig. 1 shows the lensing power spectrum calculated from CAMB compared to the lensing power spectrum calculated within the Limber approximation. We see the agreement is very good for $\ell \gtrsim 20$, since the width of the kernel is much larger than the wavelength of the modes which dominate the signal on these scales. In order to understand the influence of the growth function $g(a)$, we also calculated the lensing power spectrum by setting $g(a) \equiv 1$. The growth function makes a difference only for $\ell \lesssim 50$. This is because for large ℓ the major contribution to $C_\ell^{\phi\phi}$ comes from midway between the last scattering surface and the observer, which is well within the matter dominated era when the growth function $g(a)$ is close to unity. We are now ready to understand the impact of the matter density on $C_\ell^{\phi\phi}$.

4 THE DEPENDENCE OF LENSING POWER SPECTRUM ON MATTER DENSITY

Eqs. (1, 6) show that there are several ways that ω_m impacts $C_\ell^{\phi\phi}$: through the primordial amplitude, A_s, the transfer function, $T(k)$, and the growth function, $g(a)$. We will see that most of the dependence comes from the transfer function, i.e. from the decay of the potentials between horizon crossing and matter-radiation equality.

4.1 Qualitative Analysis

Defining $x = \chi/\chi_\star$, the lensing power spectrum can be written as

$$\ell^4 C_\ell^{\phi\phi} \simeq A_s \chi_\star \int_0^1 \mathrm{d}x\; kT^2\left(\frac{\ell}{x\chi_\star}\right)(1-x)^2 g^2(a), \qquad (7)$$

where $a = a(x)$, we have dropped all constant factors and we have adopted $n_s = 1$.

We can now gain some insight by plotting in Fig. 2 the various factors in this integrand for two values of ℓ, one on each side of the $\ell^4 C_\ell^{\phi\phi}$ peak ($\ell \simeq 50$). Let's consider the $\ell = 800$ case first. Recalling $\chi_\star \sim 10^4$ Mpc we

see the power spectrum (the kT^2 factor, which peaks at $k \sim k_{\rm eq} \sim 10^{-2}\,{\rm Mpc}^{-1}$) is monotonically rising as the comoving distance, x, increases and we probe power at longer wavelengths (smaller k). Since the lensing kernel is dropping the net result is a broad integrand with a peak at about 40% of the way back to last scattering. Very little power comes from times when the growth function is significantly different from unity. All dependence of the lensing kernel on ω_m has been pulled out into the prefactor of the integrand which, as we shall see, has only a weak dependence on ω_m. The bulk of the dependence then comes from the transfer function.

In contrast, for the $\ell = 20$ case we can see that the turnover of the matter power spectrum (the drop in power at $k < k_{\rm eq}$) becomes very important, reducing contributions from large comoving distance. In this case the growth factor and its dependence on the matter density cannot be neglected.

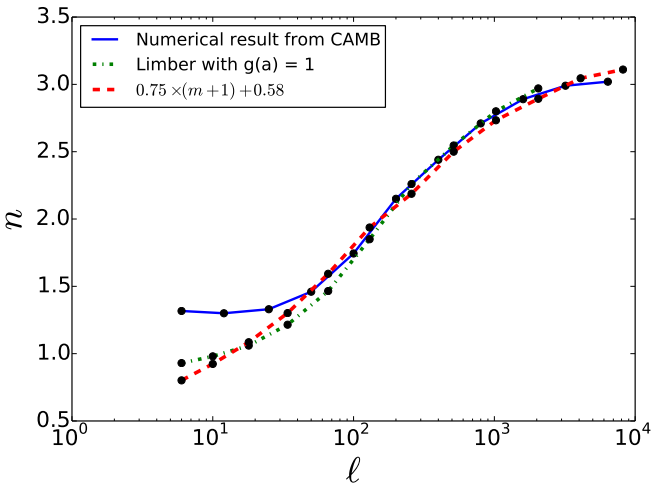

Figure 3. The dependence of the lensing power spectrum on the matter density, $\ell^4 C_\ell^{\phi\phi} \sim (\omega_m)^n$. The solid line is the numerical result from CAMB, the dashed line is the result of the analytic scaling law derived in the text ($n = 0.75(m+1) + 0.58$) and the dash-dotted line is the result of the Limber approximation setting $g(a) = 1$.

4.2 Quantitative Analysis

To provide a quantitative test of our understanding we calculate the dependence of $C_\ell^{\phi\phi}$ on ω_m. We begin by assuming a power-law matter power spectrum and set the growth function to 1. These assumptions allow us to calculate the dependence analytically, and they are a good approximation for $\ell > \ell_{\rm eq} = k_{\rm eq}\chi_\star \simeq 140$. We shall then include the physical transfer function and finally the growth function.

We begin by determining the dependence of the prefactor in Eq. (7), $A_s\chi_*$, on ω_m. A sample of ΛCDM models from WMAP9 chains gives the following scaling relations

$$A_s \propto \omega_m^{0.58} \quad , \quad \chi_\star\theta_\star \propto \omega_m^{-0.25} \tag{8}$$

where $\theta_\star$ is the angular size of the sound horizon at recombination, which is well determined by the WMAP9 data and is almost independent of ω_m. We also find the power law index n_s is close to uncorrelated with ω_m, so it is safe to set $n_s = 1$ as we have been doing.

The scaling of A_s with ω_m comes directly from the "potential envelope" effect described in Section 2. For the acoustic peak region the potential envelope of Hu & White (1997) is well fit by $\omega_m^{-0.58}$ so $A_s \propto \omega_m^{0.58}$ keeps the power in the acoustic peaks consistent with the data.

The scaling of $\chi_\star$ with ω_m arises from the dependence of the sound horizon on the expansion rate near last scattering. If we assume $z_\star$ is fixed, and if we were to neglect the contribution of radiation to the expansion rate, then the sound horizon (r_s) would scale as $\omega_m^{-1/2}$. The presence of radiation softens this dependency to $\omega_m^{-0.25}$ (Hu et al. 2001). With $\theta_\star$ so well determined from the data, $\chi_\star = r_s/\theta_\star$ has the same scaling as r_s.

The matter power spectrum $P_\delta(k) \sim kT^2(k)$ which we shall approximate locally as a power law

$$P_\delta(k) \sim kT^2(k) \sim k\left(\frac{k_{\rm eq}}{k}\right)^{m+1} = \frac{k_{\rm eq}^{m+1}}{k^m} \quad . \tag{9}$$

The scaling with $k_{\rm eq}$ is due to the suppression of the potential that occurs between horizon crossing and the onset of matter domination.

We can now derive the dependence of $C_\ell^{\phi\phi}$ on ω_m:

$$\begin{aligned} \ell^4 C_\ell^{\phi\phi} &\sim A_s \frac{(k_{\rm eq}\chi_\star)^{m+1}}{\ell^m} \int_0^1 {\rm d}x\; x^m(1-x)^2 g^2(a) \\ &\sim \omega_m^{0.75(m+1)+0.58}\ell^{-m} \int_0^1 {\rm d}x\; x^m(1-x)^2 g^2(a) \\ &= \omega_m^{0.75(m+1)+0.58}\ell^{-m}\; f(\omega_m), \end{aligned} \tag{10}$$

where we have denoted the final integral as $f(\omega_m)$ and the ω_m dependence comes from the growth function, g. Since the dependence of $g(a)$ on ω_m is strong only in the late universe where, as we have seen, the integrand is very small the dependence of $f(\omega_m)$ on the matter density is weak and we finally obtain the scaling law

$$\ell^4 C_\ell^{\phi\phi} \sim \omega_m^{0.75(m+1)+0.58}\; \ell^{-m}. \tag{11}$$

Of course the power spectrum is not well approximated by a single power-law. We compute the local power-law index, m, numerically by matching the numerically-determined $\ell^4 C_\ell^{\phi\phi}$ to ℓ^{-m}. Using this m our analytic result for the scaling of $\ell^4 C_\ell^{\phi\phi}$ with ω_m is very accurate for $\ell > \ell_{\rm eq}$, as we show in Fig. 3.

We now demonstrate that the failure of the above prediction for $n(\ell)$ at $\ell \lesssim 50$ is mostly due to neglecting the growth factor. We do so by showing how the agreement with the numerical result improves dramatically at $\ell \lesssim 50$ if we compare to the numerical result with $g(a)$ set to unity. Reducing ω_m leads to an increase in Ω_Λ in order to keep the angular size of the sound horizon fixed, which in turn leads to a decrease in $g(a)$. Thus including the growth factor increases $n(\ell)$ over the range in ℓ where the growth factor is important.

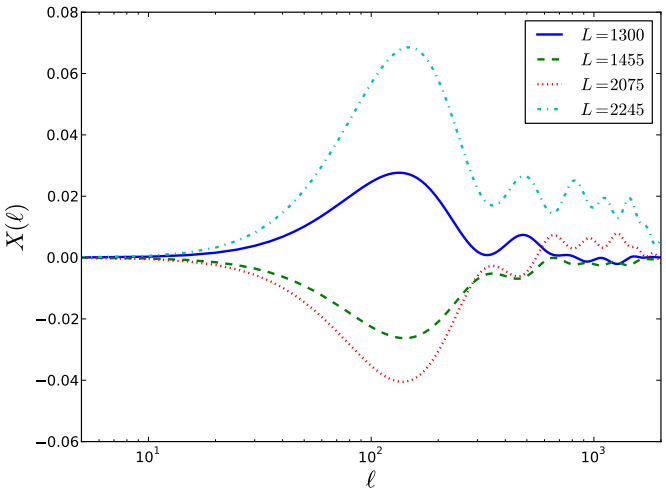

Figure 4. The contribution of each multipole of the CMB lensing power spectrum, $C_\ell^{\phi\phi}$ to the lensing of the CMB temperature power spectrum, C_L^{TT}, assuming our fiducial cosmology (WMAP9 best-fit ΛCDM model), for two values of L near acoustic peaks (1455 and 2075), and two values near troughs (1300 and 2245).

5 DISCUSSION

Precise measurements of anisotropies on small angular scales allow tight constraints on the matter density due to its impact on the amplitude of gravitational lensing of the angular power spectrum of temperature anisotropies (Hou et al. 2014). Within the context of ΛCDM models we found that this dependence on the matter density arises mainly from the dependence of $P_\Phi(k)$ on ω_m.

The origin of the dependence of $P_\Phi(k)$ on ω_m is well understood (Kodama & Sasaki 1984; Peacock 1999; Liddle & Lyth 2000; Dodelson 2003), and arises from the decay of the potential that occurs after horizon crossing but before matter-radiation equality. Increasing ω_m increases $z_{\rm eq}$ and thereby decreases the amount of this decay.

Other sources of dependence (the lensing kernel, the correlation between A_s and ω_m and the growth function) contribute in a subdominant manner. The growth factor is only important at $\ell \lesssim \mathbf{50}$. On such large angular scales the turnover of the matter power spectrum suppresses contributions from earlier times, thereby making nearby contributions relatively more important.

This brings up the question, how much does $\ell < 50$ contribute to the lensing of the temperature power spectrum? To answer it we define $X(\ell)$ via $(C_L^{TT} - C_{L\ \rm unlensed}^{TT})/C_{L\ \rm unlensed}^{TT} = \int X(\ell) d\ln\ell$ (using Eq.(4.12) of Lewis & Challinor (2006)) and plot the integrand in Fig. 4 for several values of L. For our fiducial ΛCDM cosmology, we see that $\ell < 50$ contributes a subdominant portion to these integrals. Setting $C_\ell^{\phi\phi}$ to zero at $\ell < 50$ changes the lensed C_ℓ^{TT} by less than 0.7% at all ℓ with peak effect at $\ell \approx 2240$. For comparison, setting $C_\ell^{\phi\phi}$ to zero at all ℓ (i.e., turning off lensing) changes the lensed C_ℓ^{TT} by about 11% at $\ell \approx 2240$. Thus the lensing of the CMB temperature power spectrum has some sensitivity to the response of $g(a)$ to changes in ω_m, but this effect is subdominant to the main effect of the response of $P_\Phi(k)$ to changes in ω_m.

We note that recent measurements of C_ℓ^{TT} at high ℓ have led to small, but important, shifts in cosmological parameters (Planck Collaboration XVI 2013). Assuming the minimal, six-parameter ΛCDM model, estimates of the matter density have gone up (and estimates of H_0 have gone down) with the inclusion of high ℓ data from Planck. When the Planck data are restricted to the angular scales well-measured by WMAP these shifts largely disappear (Planck Collaboration XVI 2013) suggesting that the parameter shifts are due to the influence of the new data at small angular scales. As Hou et al. (2014) point out, the impact of lensing on the CMB temperature power spectrum provides some of the sensitivty to ω_m for the high ℓ data. With this work we now understand the physical origin of that dependence on ω_m.

6 ACKNOWLEDGMENTS

Z.P. would like to thank Brent Follin and Marius Millea for sharing codes. M.W. is supported by NASA. This work made extensive use of the NASA Astrophysics Data System and of the `astro-ph` preprint archive at `arXiv.org`.

REFERENCES

Carlstrom J. E. et al., 2011, PASP, 123, 568
Dodelson S., 2003, Modern cosmology
Hinshaw G. et al., 2013, ApJs, 208, 19
Hou Z. et al., 2014, ApJ, 782, 74
Hu W., Dodelson S., 2002, ARA&A, 40, 171
Hu W., Fukugita M., Zaldarriaga M., Tegmark M., 2001, ApJ, 549, 669
Hu W., White M., 1996, ApJ, 471, 30
Hu W., White M., 1997, ApJ, 479, 568
Kodama H., Sasaki M., 1984, Progress of Theoretical Physics Supplement, 78, 1
Lewis A., Challinor A., 2006, Phys.Rep, 429, 1
Liddle A. R., Lyth D. H., 2000, Cosmological Inflation and Large-Scale Structure
Limber D. N., 1953, ApJ, 117, 134
Peacock J. A., 1999, Cosmological Physics
Planck Collaboration I, 2011, A&A, 536, A1
Planck Collaboration I, 2013, Submmited to A&A
Planck Collaboration XVI, 2013, Submmited to A&A
Seljak U., Sugiyama N., White M., Zaldarriaga M., 2003, Phys.Rev.D, 68, 083507
Sievers J. L. et al., 2013, J. of Cosm.& Astropart., 10, 60